Check for updates

IGF-IR tyrosine kinase interacts with NPM-ALK oncogene to induce survival of T-cell ALK$^+$ anaplastic large-cell lymphoma cells

Ping Shi,[1] Raymond Lai,[2] Quan Lin,[1] Abid S. Iqbal,[1] Leah C. Young,[3] Larry W. Kwak,[4] Richard J. Ford,[1] and Hesham M. Amin[1]

[1]Department of Hematopathology, The University of Texas M. D. Anderson Cancer Center, Houston; Departments of [2]Laboratory Medicine and Pathology and [3]Medical Genetics, The University of Alberta, Edmonton, AB; and [4]Department of Lymphoma and Myeloma, The University of Texas M. D. Anderson Cancer Center, Houston

Type I insulin-like growth factor receptor (IGF-IR) tyrosine kinase plays important roles in the pathogenesis of several malignancies. Although it promotes the growth of stimulated hematopoietic cells, a direct role of IGF-IR in malignant lymphoma has not been identified. Anaplastic lymphoma kinase-positive anaplastic large-cell lymphoma (ALK$^+$ ALCL) is a unique type of T-cell lymphoma. Approximately 85% of ALK$^+$ ALCL cases harbor the translocation t(2;5)(p23;q35), which generates the chimeric oncogene NPM-ALK. In the present study, we explored a possible role of IGF-IR in ALK$^+$ ALCL. Our results demonstrate that IGF-IR and IGF-I are widely expressed in ALK$^+$ ALCL cell lines and primary tumors. Importantly, we identified novel reciprocal functional interactions between IGF-IR and NPM-ALK. Antagonism of IGF-IR decreased the viability, induced apoptosis and cell-cycle arrest, and decreased proliferation and colony formation of ALK$^+$ ALCL cell lines. These effects could be explained by alterations of cell survival regulatory proteins downstream of IGF-IR signaling. Our findings improve current understanding of the biology of IGF-IR and NPM-ALK and have significant therapeutic implications as they identify IGF-IR signaling as a potential therapeutic target in ALK$^+$ ALCL and possibly other types of malignant lymphoma. (Blood. 2009;114:360-370)

Introduction

Type I insulin-like growth factor receptor (IGF-IR) is a tetrameric transmembrane receptor tyrosine kinase that is composed of 2 α and 2 β subunits linked by disulfide bonds.[1] The activation of IGF-IR is primarily mediated through its mitogenic ligands IGF-I and, to a lesser degree, IGF-II. In addition, IGF-IR shows much lower affinity to insulin.[2] Ligand binding to IGF-IR activates its intrinsic tyrosine kinase activity, which leads to *trans*-β subunit autophosphorylation and subsequent stimulation of major signaling cascades including IRS-1/PI-3K/Akt/FKHR, Grb/Ras/MAPK, and JAK/STAT.[3-8] Signaling through IGF-IR contributes to the development of human malignancies and to the proliferation and viability of their cells. The ability of IGF-IR to induce transformation and mitogenesis and to promote cell survival has been shown by using in vitro and in vivo experimental models.[9-11] Furthermore, IGF-IR plays important roles in regulating cell differentiation, shape and migration, and metastatic potential.[12-17] These effects have been demonstrated in solid tumors including those of the prostate, breast, colon, lung, and neural tissues.[18-24] As clinical trials are currently underway, it is anticipated that selective or specific antagonism of IGF-IR signaling will be used for the treatment of some of these malignancies in the near future.[2,25-28]

Previous studies have documented that IGF-IR is also expressed in hematopoietic cells and in some myeloid and lymphoid neoplastic cells.[29] IGF-I/IGF-IR signaling is required for the proliferation and cytokine-independence of stimulated hematopoietic cells.[29-32] Despite these important observations, few studies have explored the role of IGF-IR in hematologic malignancies, and the overwhelming majority of these studies focused on plasma cell myeloma.[33-35] To our knowledge, a specific role of IGF-IR has yet to be identified in malignant lymphoma.

Anaplastic lymphoma kinase (ALK) is a transmembrane receptor tyrosine kinase that belongs to the insulin receptor superfamily. The physiologic expression of ALK is exclusively restricted to embryonic cells of neural origin, which suggests that ALK may play a role in the development of neural tissues.[36,37] In a unique type of T-cell lymphoma, identified by the World Health Organization classification scheme as anaplastic large-cell lymphoma (ALCL), ALK-positive (ALK$^+$), ALK is expressed and constitutively activated because of one of several chromosomal aberrations involving the *ALK* gene on chromosome 2p23.[38] The translocation t(2;5)(p23;q35), which also involves the *NPM* (nucleophosmin) gene, constitutes approximately 85% of these aberrations. One major outcome of this translocation is the generation of the NPM-ALK chimeric protein and a constitutively active ALK.[39,40] ALK$^+$ ALCL is an aggressive type of malignant lymphoma that frequently affects children and young adults.[41,42] The patients usually present with widespread systemic disease and B symptoms. After an initial response to the current combination chemotherapy cyclophosphomide, adriamycin, vincristine, and prednisone (CHOP)–based therapy, 30% to 40% of the patients have a relapse, and subsequent death is not uncommon.[43-45]

NPM-ALK induces significant oncogenic effects,[46] but the exact mechanisms involved are not completely understood. NPM-ALK associates and functionally interacts with an array of molecules known to regulate cell survival and growth such as IRS-1/PI-3K/Akt/FKHR and JAK/STAT.[47] Because ALK demonstrates structural homology with

Submitted November 21, 2007; accepted April 26, 2009. Prepublished online as *Blood* First Edition paper, May 7, 2009; DOI 10.1182/blood-2007-11-125658.

The online version of this article contains a data supplement.

The publication costs of this article were defrayed in part by page charge payment. Therefore, and solely to indicate this fact, this article is hereby marked "advertisement" in accordance with 18 USC section 1734.

© 2009 by The American Society of Hematology

Downloaded from http://ashpublications.net/blood/article-pdf/114/2/360/1319577/zh802809000360.pdf by guest on 12 June 2024

IGF-IR, and several downstream survival molecules are shared between the 2 kinases, we explored whether ALK$^+$ ALCL cells express IGF-IR. We also investigated possible functional interactions between IGF-IR and NPM-ALK kinases and whether IGF-IR signaling directly contributes to the survival of this type of aggressive malignant lymphoma.

Methods

Antibodies

Details are included in the supplemental methods (available on the *Blood* website; see the Supplemental Materials link at the top of the online article).

Cell lines, cell cultures, and treatments

Five ALK$^+$ ALCL cell lines—Karpas 299, SU-DHL-1, SUP-M2, SR-786, and DEL—were used. The P6 (mouse BALB/c3T3 fibroblasts overexpressing human IGF-IR) and R$^-$ (mouse 3T3-like fibroblasts with targeted ablation of *Igf1r*) cell lines were a generous gift from Dr R. Baserga (Thomas Jefferson University, Philadelphia, PA) and were used as positive and negative controls, respectively, for the expression of IGF-IR.[48,49] The plasma cell myeloma EJM cell line (DSMZ) and the spontaneously immortalized Schwann cells RSC96 (ATCC) were used as positive and negative controls, respectively, for the expression of IGF-I. The human fibroblast cell line AG01523 (Coriell Institute for Medical Research) was used as a negative control for picropodophyllin (PPP) effect.[34] In addition, Jurkat (provided by Dr J. Chandra, The University of Texas M. D. Anderson Cancer Center, Houston, TX) and 293T (ATCC) cell lines were used in transfection experiments. The ALK-negative ALCL cell line Mac-2A (provided by Dr G. Rassidakis, The University of Texas M. D. Anderson Cancer Center, Houston, TX) was used in some of the experiments. Cell lines were maintained in RPMI 1640 (ALK$^+$ ALCL and Jurkat cell lines), Dulbecco modified Eagle medium (DMEM; P6, R$^-$, RSC96, 293T), Iscove modified Dulbecco medium (IMDM; EJM), or Eagle minimum essential medium in Earle balanced salt solution (EEMEM; AG01523) supplemented with 10% fetal bovine serum (FBS; 15% FBS for AG01523 and Mac-2A; Sigma-Aldrich), 2 mM glutamine, 100 U/mL penicillin, and 100 μg/mL streptomycin at 37°C in humidified air with 5% CO_2. Normal human peripheral blood pan T cells were from Allcells (PB009.1F).

Selective targeting of IGF-IR was achieved by using the cyclolignan PPP (Clontech) dissolved in ethanol to a concentration of 0.5 mM (final concentration of ethanol was less than 0.4% by volume). In some experiments, cells were treated with recombinant human IGF-I (291-G1-050; R&D Systems) after being cultured in serum-free medium for 3 hours (viability, migration, and apoptosis analysis) or overnight (kinase assay). Then, 500 ng/mL IGF-I were added with/without anti–IGF-I neutralizing antibody or anti-IGF-IR blocking antibody at concentrations of 2.5 or 5 μg/mL, respectively.

Excluding 293T cells, electroporation was used to transfect small interfering RNA (siRNA) or plasmids. Transfection of 293T cells was performed using Lipofectamine 2000 (Invitrogen). Specific targeting of *IGF-IR* or *ALK* was achieved by transient transfection with SMARTpool-designed siRNA (mixture of 4 different constructs). The siCONTROL Non-Targeting siRNA was used as a negative control (Dharmacon). Transfection of the cells by siRNA or plasmids was performed using the Nucleofector "V" solution as recommended by the manufacturer (Amaxa Biosystems; A-030 program for ALK$^+$ ALCL, T-030 for P6 and R$^-$, and X-001 for Jurkat cell lines).

Expression plasmids

Full-length *NPM-ALK* (amino acids 1-680) in pCDNA3.1(+) was mutated to generate the K210A, Y338F, Y567F, Y644F, Y646F, and Y664F mutants by using the QuickChange II XL site-directed mutagenesis kit (200521-5; Stratagene) according to the manufacturer's instructions. To prepare deletion mutants of *NPM-ALK* (NPM-ALK/98-680 and NPM-ALK/98-566), primers NPM-ALK-*Hin*dIII/ATG-F (5′-CCAAGCTTATGGTGGTCT-TAAGGTTGAA-3′) and *NPM-ALK-Xho*1/ACT1-R (5′-AACTCGAGT-CAGGGCCCAGGCTGGTTCA-3′) or NPM-ALK-*Xho*1/ACT2-R (5′-AACTCGAGTCACGTTGGGTTCCACAAGCTGGTTT-3′) were used to amplify portions of *NPM-ALK*, which subsequently were digested with *Hin*dIII/*Xho*1 and subcloned into pCDNA3.1(+). The human IGF-IR containing a complete open reading frame in pBluescriptII KS(+) (gift from Dr D. LeRoith, Mount Sinai School of Medicine, New York, NY) was subcloned into the *Eco*R1 and *Not*1 sites of pCDNA3.1(+). The mutation Y1131,1135,1136F of IGF-IR kinase domain was generated using a similar approach. Mutant DNA was sequenced using ABI 3730*xl* Genetic Analyzer (Applied Biosystems). The NPM-ALK^{K210R} plasmid was provided by Dr G. Rassidakis.

Relative antigen density of IGF-IR

Details are included in the supplemental methods.

Cell viability and proliferation assays

Details are included in the supplemental methods.

Apoptosis detection

Details are included in the supplemental methods.

Cell-cycle analysis

Details are included in the supplemental methods.

Cell migration assay

Details are included in the supplemental methods.

Colony formation in soft agar

Details are included in the supplemental methods.

Autocrine release of IGF-I

Details are included in the supplemental methods.

Reverse transcription polymerase chain reaction

Total RNA was isolated using the RNeasy Mini kit (QIAGEN). Reverse transcription (RT) was performed using the One-Step RT-PCR kit (QIAGEN). IGF-IRα, IGF-IRβ, and IGF-I primers and the polymerase chain reaction (PCR) conditions are shown in Table 1. Two different sets of IGF-I primers were used for confirmation. Amplification was performed in a PTC100 thermal cycler (MJ Research). β-Actin (RDP-38; R&D Systems) was used as control. The PCR products were detected by ethidium bromide staining on a 1% agarose gel and visualized using the FluorChem 8800 imaging system (Alpha Innotech).

Tyrosine kinase activity

Details are included in the supplemental methods.

Immunoprecipitation and Western blot analysis

Cell lysates were obtained using standard techniques (lysis buffer detail is included in the supplemental methods). For immunoprecipitation, lysates were incubated with primary antibody overnight at 4°C. Agarose beads conjugated with A/G were then added and incubated for 2 hours at 4°C. The immunocomplexes were spun, washed 3 times with cold phosphate-buffered saline (PBS) and once with lysis buffer, and then subjected to sodium dodecyl sulfate–polyacrylamide gel electrophoresis (SDS-PAGE). For Western blotting (WB), 50- to 80-μg total proteins were electrophoresed on 6% to 12% SDS-PAGE. The proteins were transferred to nitrocellulose membranes and probed with specific primary antibodies and then with the appropriate horseradish peroxidase–conjugated secondary antibodies (Santa Cruz Biotechnology and GE Healthcare). Proteins were detected using a chemiluminescence-based kit (GE Healthcare).

Downloaded from http://ashpublications.net/blood/article-pdf/114/2/360/1319577/zh802809000360.pdf by guest on 12 June 2024

Table 1. *IGF-IRα*, *IGF-IRβ*, and *IGF-I* primers and PCR conditions

Primers and conditions	
***IGF-IRα* (product size 307 bp)**	
Forward	5′-GTAGCTTGCCGCCACTACTACT-3′
Reverse	5′-GGAGCATCTGAGCAGAAGTAACAGA-3′
Amplification (35 cycles)	94°C (30 seconds), 58°C (30 seconds), 72°C (30 seconds)
Final elongation	72°C (10 minutes)
***IGF-IRβ* (product size 450 bp)**	
Forward	5′-TGGGGAAGGAGTGCTGTAT-3′
Reverse	5′-CGGCCATCTCTGAATCATCTTG-3′
Amplification (35 cycles)	94°C (60 seconds), 56°C (60 seconds), 72°C (60 seconds)
Final elongation	72°C (10 minutes)
***IGF-I* (product size 413 bp)**	
Forward	5′-TCCTCGCATCTCTTCTACC-3′
Reverse	5′-TGGCATGTCACTCTTCACT-3′
Amplification (35 cycles)	94°C (60 seconds), 58°C (60 seconds), 72°C (60 seconds)
Final elongation	72°C (10 minutes)
***IGF-I* (product size 299 bp)**	
Forward	5′-GAAGGTGAAGATGCACACCA-3′
Reverse	5′-AGCGAGCTGACTTGGCAGGCTTGA-3′
Amplification (35 cycles)	94°C (60 seconds), 63°C (40 seconds), 72°C (60 seconds)
Final elongation	72°C (10 minutes)

STAT3 and FKHR binding to DNA

STAT3 or FKHR binding to DNA was examined using an electrophoretic mobility shift assay (EMSA) technique and commercially available kits (Panomics). Nuclear extracts were prepared from 2×10^6 cells using the Nuclear Extract kit (Panomics). Then, 1 μg poly(dI-dC) and 10 ng biotin-labeled STAT3 or FKHR probe were added to 5 μg nuclear extract and incubated in binding buffer at 20°C for 30 minutes. For the supershift analysis, specific antibody at 1 μg/reaction was incubated with the nuclear proteins on ice for 20 minutes before labeled oligonucleotide was added. The mixtures were separated on 6% nondenaturing PAG and subsequently transferred to nylon membranes. After blocking, the membranes were incubated with streptavidin-horseradish peroxidase conjugate. Detection was performed, and the shifted bands corresponding to STAT3-DNA or FKHR-DNA complex were visualized relative to the unbound double-stranded DNA. In addition, 5 μg nuclear extracts were used for assessing the binding of STAT3 or FKHR to DNA using the TransAM enzyme-linked immunosorbent assay (ELISA) kits (45 196 for STAT3 and 46 396 for FKHR; Active Motif) according to the manufacturer's instructions.

Patients, tissue microarray, and immunohistochemical staining

Details are included in the supplemental methods. These studies were approved by the ethical research committee at Cross Cancer Institute, and all patients provided informed consent in accordance with the Declaration of Helsinki.

Statistical analysis

Statistical analysis was performed using Student *t* test for paired data or 2-way analysis of variance (ANOVA) and Bonferroni post hoc test, where appropriate, in Prism 5 for Mac OS X software version 5.0b (GraphPad Software). A *P* value less than .05 was considered statistically significant.

Results

Expression of IGF-IR and IGF-I by ALK$^+$ ALCL cell lines and tumors

To explore the expression of IGF-IR protein and mRNA in 5 ALK$^+$ ALCL cell lines, we used immunohistochemical staining, WB, and RT-PCR. All ALK$^+$ ALCL cell lines demonstrated significant levels of IGF-IR protein and mRNA (Figure 1A-C). P6 and R$^-$ cell lines were used as positive and negative controls, respectively. Interestingly, the R$^-$ cells that we used as a negative control for IGF-IR demonstrated low levels of expression of the IGF-IRβ subunit mRNA, but were entirely negative for the IGF-IRα subunit mRNA (Figure 1C). These cells were originally developed in mice after targeted ablation of *Igf1r*.[48] In agreement with our observations, a recent study showed that some R$^-$ cell subclones might express low levels of IGF-IRβ.[50] We also performed quantitative analysis of IGF-IR expression using flow cytometry. As shown in Figure 1D, the ALK$^+$ ALCL cell lines demonstrated remarkably higher levels of expression of IGF-IR compared with normal human T lymphocytes. R$^-$ and P6 cells were used as negative and positive controls, respectively.

Similar techniques were used to explore the expression of IGF-I. EJM and RSC96 cells were used as positive and negative controls, respectively. All of the ALK$^+$ ALCL cell lines except

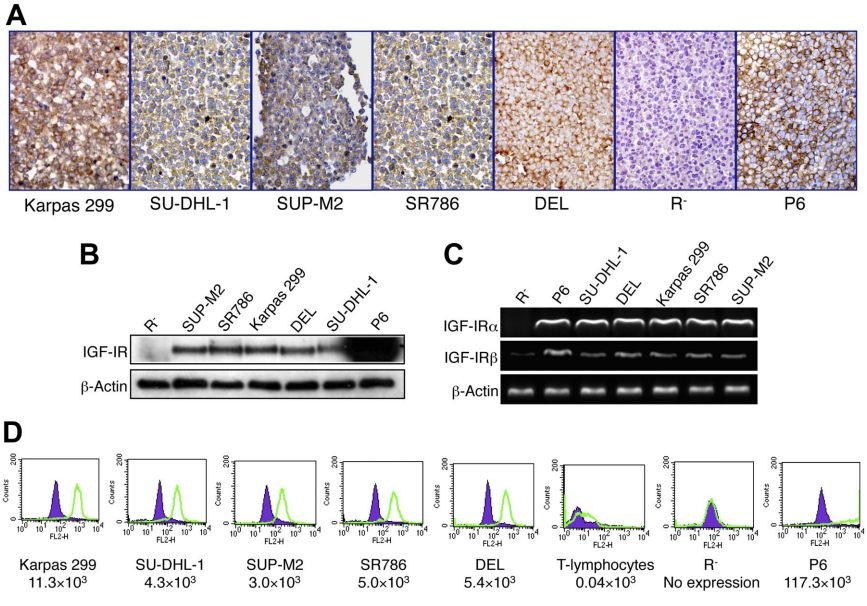

Figure 1. Expression of IGF-IR by ALK$^+$ ALCL cell lines. (A) Immunohistochemical staining demonstrates the expression of IGF-IR protein in 5 ALK$^+$ ALCL cell lines: Karpas 299, SU-DHL-1, SUP-M2, SR786, and DEL. The cell lines R$^-$ and P6 were used as negative and positive controls, respectively. The expression of IGF-IR is limited to the cell membrane and cytoplasm, whereas the nuclei are negative (original magnification, ×400). (B) WB studies confirm the results. It is important to note that the overexpression of IGF-IR in P6 cells does not represent a physiologic level. (C) RT-PCR shows the presence of IGF-IR mRNA in the ALK$^+$ ALCL cell lines as well as in the P6 cell line. Although IGF-IRα mRNA is not detectable in R$^-$ cells, these cells appear to express very low levels of IGF-IRβ mRNA. (D) Quantitative flow cytometric analysis shows that the ALK$^+$ ALCL cell lines express significantly higher levels of IGF-IR compared with normal human T lymphocytes. R$^-$ and P6 cell lines were used as negative and positive controls for the expression of IGF-IR, respectively. The estimated numbers of IGF-IR molecules/cell are shown.

Downloaded from http://ashpublications.net/blood/article-pdf/114/2/360/1319577/zh802809000360.pdf by guest on 12 June 2024

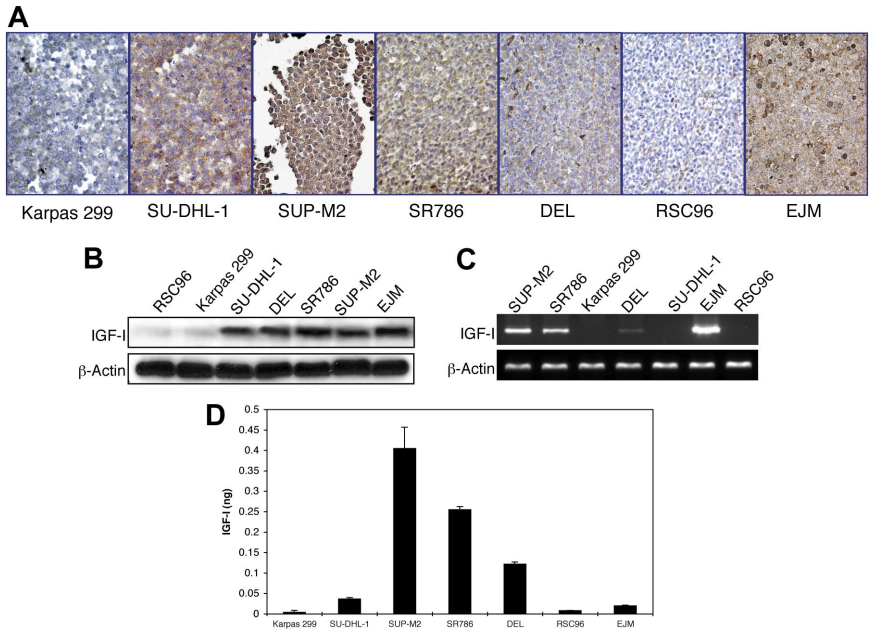

Figure 2. Expression of IGF-I by ALK+ ALCL cell lines. (A) Immunohistochemical staining of ALK+ ALCL cell lines demonstrates the expression of IGF-I in 4 cell lines: SU-DHL-1, SUP-M2, SR786, and DEL. Karpas 299 cells are negative for IGF-I. RSC96 and EJM cells served as negative and positive controls, respectively. The expression of IGF-I is cytoplasmic, and the cell membranes and nuclei are negative (×400). (B) WB shows similar findings. (C) RT-PCR shows the presence of IGF-I mRNA in SUP-M2, SR786, DEL (low level), and EJM, and its absence in Karpas 299, SU-DHL-1, and RSC96. (D) ELISA supports autocrine release of IGF-I. SUP-M2, SR786, and DEL cell lines demonstrate the presence of IGF-I in cell culture supernatants. The EJM cell line was included because it expresses IGF-I protein and mRNA. IGF-I is almost undetectable in cell culture supernatants from Karpas 299 and RSC96 cells. The experiment was repeated 3 times, and the results are shown as the mean ± SD. $P < .01$ for SUP-M2, SR786, and DEL compared with other cell lines.

Karpas 299 expressed IGF-I protein (Figure 2A-B). RT-PCR for IGF-I was performed using 2 different sets of primers to confirm the results (Figure 2C). Significant levels of IGF-I mRNA were present in SUP-M2 and SR786 cell lines. Lower levels were seen in DEL cell line (Figure 2C). Moreover, IGF-I was detected in cell culture supernatant from SUP-M2, SR786, and DEL, indicating autocrine release by these cell lines (Figure 2D). RSC96 cells and EJM cells were included because they lack or express IGF-I protein and mRNA, respectively. Although EJM and SU-DHL-1 cells expressed IGF-I protein, these cells had relatively low levels of IGF-I in cell culture supernatant (Figure 2D). These findings suggest that in certain cell types, despite high levels of expression, significant autocrine release of IGF-I may not necessarily occur.

To explore the frequency of IGF-IR and IGF-I expression in tumors from patients, we studied 12 previously characterized ALK+ ALCL primary tumors.[51] In a reactive lymph node, weak expression of IGF-IR was seen in germinal center lymphocytes, with more pronounced expression in lymphocytes and plasma cells in the mantle zone (Figure 3A). The expression of IGF-IR was present in a majority representing 10 of 12 (83%) ALK+ ALCL tumors. Two positive cases are shown in Figure 3B-C. Weak expression of IGF-I was limited to a few scattered lymphocytes in the reactive lymph node (Figure 3D). IGF-I was detected in 8 of 12 (67%) tissue samples; Figure 3E-F depicts 2 examples of positive cases, and Figure 3G-H shows 2 negative cases.

We also studied the expression of IGF-IR and IGF-I proteins in primary specimens from ALK-negative ALCL patients (supplemental

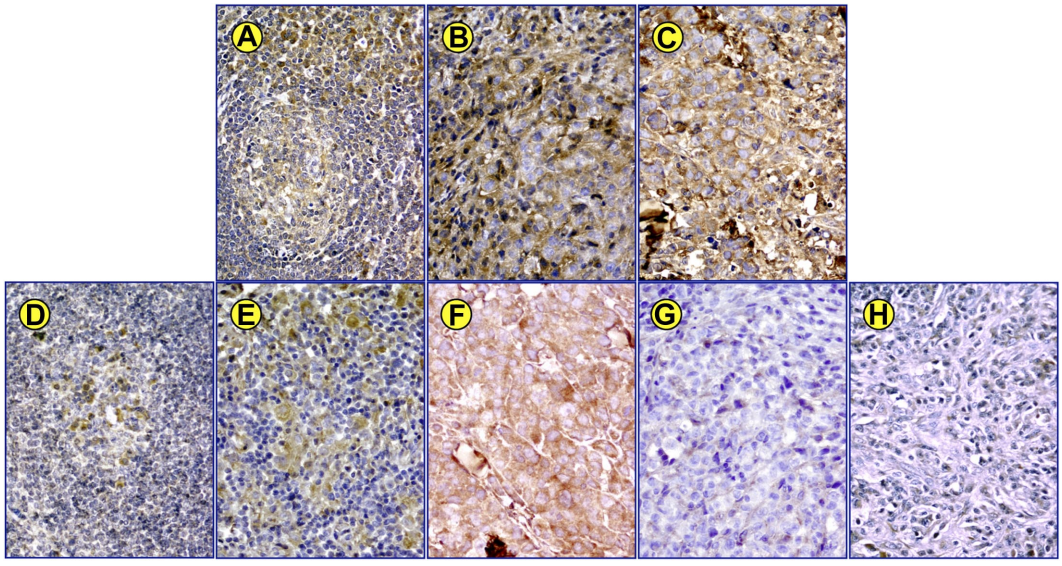

Figure 3. Expression of IGF-IR and IGF-I in primary tumors from ALK+ ALCL patients. (A) Immunohistochemical staining of sections from a reactive lymph node shows that IGF-IR is weakly expressed in germinal center lymphocytes. The expression of IGF-IR is more pronounced in small lymphocytes and plasma cells in the mantle zone (×400). Of 12 ALK+ ALCL tumor samples, 10 demonstrated significant levels of expression of IGF-IR. Examples of 2 positive tumors are shown in panels B and C. (D) Immunohistochemical study of a reactive lymph node shows very low levels of expression of IGF-I in scattered small lymphocytes and plasma cells. Eight of 12 ALK+ ALCL tumors showed the expression of IGF-I. Two positive cases are illustrated in panels E and F. (E) The large infiltrating tumor cells are positive for IGF-I, and the background small benign lymphocytes are negative. (F) Lymph node architecture is replaced by tumor cells that are strongly positive for IGF-I. (G-H) Illustrated are 2 ALK+ ALCL cases where the lymphoma cells are negative for IGF-I.

Downloaded from http://ashpublications.net/blood/article-pdf/114/2/360/1319577/zh802809000360.pdf by guest on 12 June 2024

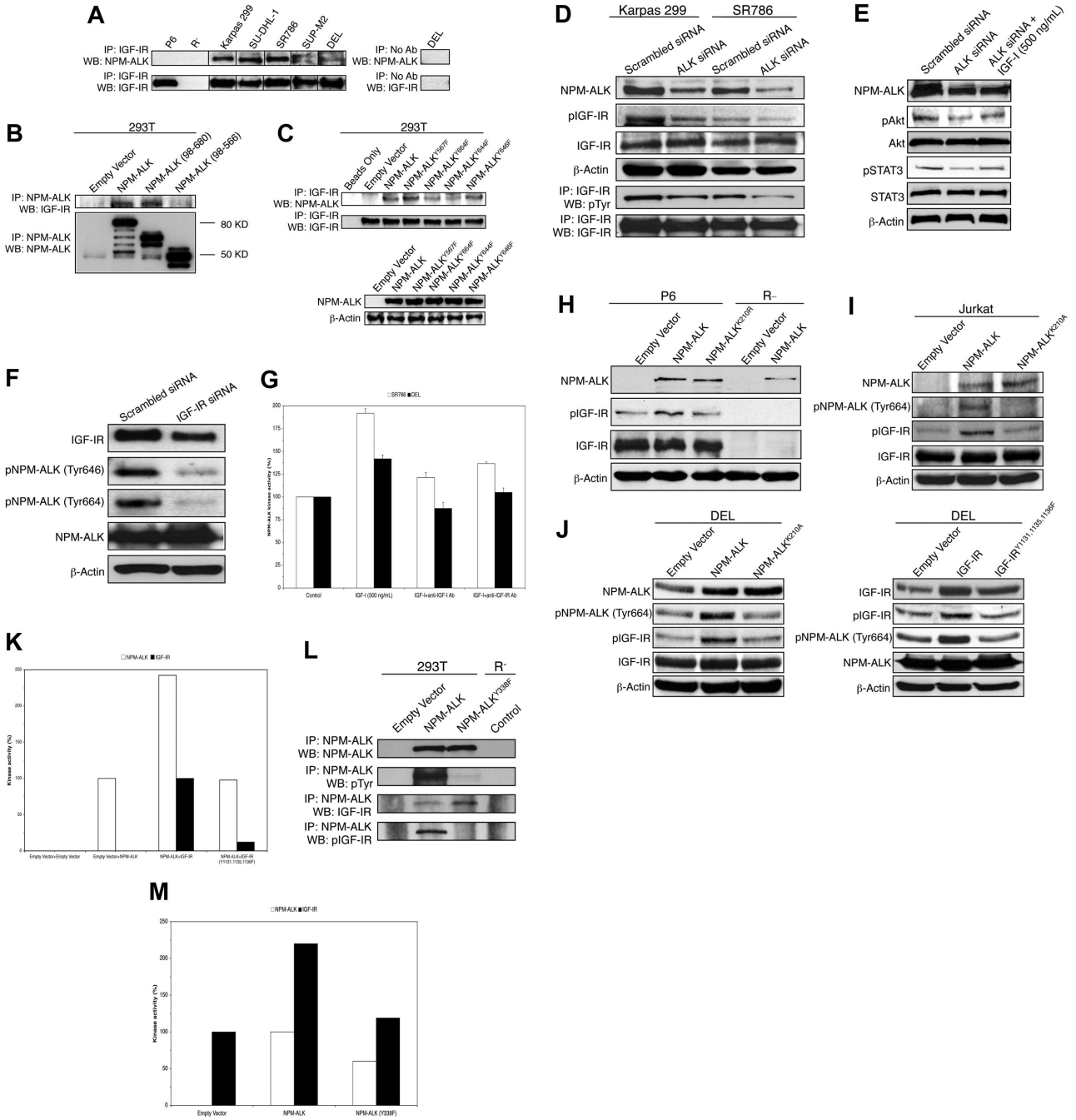

Figure 4. Physical association and reciprocal functional interactions between IGF-IR and NPM-ALK. (A left panel) Immunoprecipitation by anti-IGF-IR antibody followed by WB by anti-ALK antibody shows IGF-IR and NPM-ALK to be physically associated in 5 ALK$^+$ ALCL cell lines. P6 and R$^-$ cells were included as controls. Vertical lines have been inserted to indicate repositioned gel lanes. (A right panel) To rule out nonspecific binding of the protein of interest, a control was used in all experiments where beads were used without an antibody, and the results from the DEL cell line are shown as a representative example. (B top panel) Transfection studies in 293T cells show that the deletion of the C terminus of NPM-ALK abrogates its ability to bind to IGF-IR, whereas deletion of the NPM portion does not affect this ability, as it appears to be similar to WT NPM-ALK. (B bottom panel) Adequate protein expression of different NPM-ALK constructs after transfection into 293T cell line is shown using coimmunoprecipitation. (C top panel) Transfection experiments in 293T cells show that IGF-IR possesses much less ability to bind to NPM-ALK^{Y644F} or NPM-ALK^{Y664F} mutant compared with its ability to bind to WT NPM-ALK, NPM-ALK^{Y567F}, or NPM-ALK^{Y646F}. (C bottom panel) WB shows adequate expression of the different NPM-ALK constructs. (D) Suggesting the functional interaction between IGF-IR and NPM-ALK, specific targeting of NPM-ALK using ALK siRNA induces marked down-regulation of pIGF-IR in Karpas 299 and SR786 cells. Changes are not seen in IGF-IR. The findings are consistent when anti-IGF-IR antibody was used for immunoprecipitation followed by anti-pTyr antibody for WB. The experiment was performed in other ALK$^+$ ALCL cell lines with consistent results. (E) Although treatment of the Karpas 299 cell line with ALK siRNA induces down-regulation of pAkt and pSTAT3, this effect is diminished when the cells are additionally stimulated with IGF-IR ligand, IGF-I. (F) In support of the reciprocal functional interactions between IGF-IR and NPM-ALK, specific targeting of IGF-IR by siRNA in Karpas 299 cells induces a significant decrease in pNPM-ALK levels at Tyr646 and Tyr664. (G) Treating the ALK$^+$ ALCL cell lines with IGF-I induces significant increase in NPM-ALK kinase activity up to 92 and 42% of its baseline levels in SR786 and DEL cell lines, respectively. This effect is largely reversed when these cells are treated with IGF-I and one of the anti–IGF-I–neutralizing antibodies or the anti-IGF-IR blocking antibody. *P* less than .01 for cells treated with IGF-I compared with controls and other treatments groups. (H) To further demonstrate the functional interaction between the 2 kinases, transfection of P6 cells with WT NPM-ALK induces significant up-regulation of pIGF-IR. In contrast, changes are not noted in pIGF-IR levels when P6 cells were transfected with NPM-ALK^{K210R}. Transfection of P6 cells with different NPM-ALK constructs did not affect the baseline levels of IGF-IR. R$^-$ cells were used as a negative control for IGF-IR expression. Using the anti-ALK antibody confirmed the expression upon transfection of either the WT NPM-ALK or NPM-ALK^{K210R}. (I) Transfection of Jurkat cell line, which expresses IGF-IR, with WT NPM-ALK induces marked increase in pIGF-IR. In contrast, NPM-ALK^{K210A} fails to induce a similar effect, and pIGF-IR remains comparable with empty vector. (J left panel) WT NPM-ALK, but not NPM-ALK^{K210A}, induces up-regulation of pIGF-IR levels in the ALK$^+$ TCL cell line DEL. (J right panel) pNPM-ALK levels significantly increase after transfection of DEL

Downloaded from http://ashpublications.net/blood/article-pdf/114/2/360/1319577/zh802809000360.pdf by guest on 12 June 2024

Figure 1). IGF-IR was expressed in 3 of 5 (60%) ALK-negative tumors, but none (0 of 6) of these tumors demonstrated the expression of IGF-I. Supplemental Figure 1A-B shows examples of ALK-negative ALCL tumors that are positive and negative for IGF-IR, respectively. Supplemental Figure 1C-D shows 2 tumors that are negative for IGF-I.

Physical association and functional interactions between IGF-IR and NPM-ALK

Immunoprecipitation using anti-IGF-IR antibody, followed by WB using anti-ALK antibody, supported the physical association between IGF-IR and NPM-ALK in 5 ALK$^+$ ALCL cell lines (Figure 4A). P6 and R$^-$ cells were used as controls. As shown in supplemental Figure 2A-B, additional coimmunoprecipitation and confocal microscopy studies further illustrated the physical association and cellular colocalization of IGF-IR or pIGF-IR with NPM-ALK. This physical association was further characterized in 293T cells transfected with wild-type (WT) or deletion mutants of NPM-ALK (Figure 4B). Deletion of the NPM portion of NPM-ALK did not affect its association with IGF-IR. In contrast, IGF-IR lacked its binding ability when the C terminus of NPM-ALK was deleted. To further characterize the binding between NPM-ALK and IGF-IR, we screened all of the 4 tyrosine residues located within the C terminus of NPM-ALK. Transfection studies in 293T cells showed that IGF-IR appears to simultaneously bind to Tyr644 and Tyr664 residues of NPM-ALK (Figure 4C). The experiment was repeated 3 times with similar results.

These findings strongly suggest that IGF-IR and NPM-ALK might functionally interact. In support of this concept, specific down-regulation of ALK by siRNA decreased pIGF-IR levels (Figure 4D). In addition, treating ALK$^+$ ALCL cells with ALK siRNA decreased pAkt and pSTAT3 levels, whereas simultaneous treatment of these cells with ALK siRNA and IGF-I maintained high levels of pAkt and pSTAT3 (Figure 4E). Next, we examined the possibility that IGF-IR could function to maintain the phosphorylation status of NPM-ALK. Specific down-regulation of IGF-IR by siRNA in Karpas 299 cells decreased pNPM-ALK levels at Tyr646 and Tyr664 (Figure 4F). In addition, IGF-I, the primary ligand of IGF-IR, increased NPM-ALK kinase activity in ALK$^+$ ALCL cell lines (Figure 4G). This effect was markedly diminished when the cells were treated with IGF-I and the anti-IGF-I neutralizing antibody or anti-IGF-IR blocking antibody.

To explore whether NPM-ALK contributes to the phosphorylation/activation of IGF-IR, we transfected P6 cells, which overexpress the IGF-IR protein, with WT NPM-ALK or NPM-ALK^{K210R}. Transfection with WT NPM-ALK, but not NPM-ALK^{K210R}, induced a notable increase in pIGF-IR levels (Figure 4H). R$^-$ cells served as a negative control for IGF-IR. Densitometry showed that the increase in pIGF-IR levels was almost 100% of its baseline levels after transfecting the P6 cells with WT NPM-ALK (supplemental Figure 3). Because the NPM-ALK^{K210R} mutant might still possess minimal ability to bind to ATP, we generated the NPM-ALK^{K210A} mutant that lacks any ability to bind to ATP and used it to perform additional experiments in more pertinent neoplastic T-cell lines. In the ALK-negative T-cell line Jurkat, WT NPM-ALK induced marked increase in pIGF-IR levels, whereas NPM-ALK^{K210A} completely failed to induce similar effects, and pIGF-IR levels were comparable with its levels in Jurkat cells transfected with empty vector (Figure 4I). We also tested the reciprocal functional interactions between IGF-IR and NPM-ALK in ALK$^+$ ALCL cells. As shown in Figure 4J, transfection of DEL cell line with WT NPM-ALK significantly increased pIGF-IR. In contrast, the levels of pIGF-IR were comparable with cells transfected with empty vector or NPM-ALK^{K210A}. Using a similar approach, WT IGF-IR induced marked increase in pNPM-ALK (Tyr664), but IGF-IR^{Y1131,1135,1136F} failed to increase the basal levels of pNPM-ALK (Tyr664), and it stayed similar to its levels after transfection with empty vector. Furthermore, we demonstrated the stimulatory effect of IGF-IR on NPM-ALK kinase activity using cotransfection approach. Cotransfection of R$^-$ cells with WT IGF-IR and not IGF-IR^{Y1131,1135,1136F} induced approximately 2.5-fold increase in NPM-ALK tyrosine kinase activity (Figure 4K).

As illustrated in Figure 4L-M, transfection studies in 293T cells showed that the Tyr338 residue appears to play a crucial role in the phosphorylation/activation of IGF-IR by NPM-ALK. Although NPM-ALK^{Y338F}, similar to WT NPM-ALK, demonstrated ability to bind to IGF-IR, this mutant completely failed to phosphorylate IGF-IR or increase its kinase activity. R$^-$ cells were used as negative control.

IGF-IR signaling is important for the survival of ALK$^+$ ALCL cells

Our results thus far strongly suggest that signaling through IGF-IR plays a role in the survival of ALK$^+$ ALCL cells. To test this possibility, we selectively targeted IGF-IR using the cyclolignan PPP.[7,33,34,52] PPP induced a time- and concentration-dependent decrease in the viability of ALK$^+$ ALCL cells (Figure 5A). At 24 hours after treatment, the half maximal inhibitory concentration (IC_{50}) of PPP was 0.5 μM for SR786 and 2.0 μM for SUP-M2 and DEL. At 48 hours, IC_{50} was 0.2 μM for SR786, 0.25 μM for SUP-M2 and DEL, 0.3 μM for Karpas 299, and 0.4 μM for SU-DHL-1. Of important note is that PPP did not induce significant decrease in the viability of normal human T lymphocytes (Figure 5A). The human skin fibroblast cell line AG01523, which is known to be resistant to PPP,[34] was used as a negative control. The decrease in cell viability could be attributable to both apoptotic cell death (Figure 5B) and G_2/M-phase cell-cycle arrest (Figure 5C). The PPP-induced apoptosis and cell cycle arrest were also documented in ALK$^+$ ALCL cells and not in normal T lymphocytes through the occurrence of typical morphologic changes (supplemental Figure 4A). Furthermore, treating ALK$^+$ ALCL cell lines with PPP decreased their proliferation (Figure 5D) and abrogated their colony formation potential (Figure 5E). For control SR786 cells, the number of colonies/plate was 251.3 ± 26.3 (mean ± SD), whereas after treatment with PPP, this number decreased to 1.3 ± 0.6. For DEL, the number of the colonies/plate was 72.0 ± 7.8 and 6.9 ± 2.0 before and after treatment with PPP, respectively.

Because selective targeting using pharmacologic agents may induce nonspecific effects, we initiated experiments based on specific approaches to further confirm the direct role of IGF-IR. The decrease in ALK$^+$ ALCL cell viability and apoptotic cell death were confirmed using specific targeting of IGF-IR by siRNA (supplemental Figure 4B-C). IGF-IR siRNA increased apoptotic

cells with WT IGF-IR. Of note is that transfection of this cell line with IGF-IR^{Y1131,1135,1136F}, which possesses significantly less kinase activity compared with WT IGF-IR, does not induce a similar effect on pNPM-ALK levels. (K) Cotransfection of R$^-$ cells with WT IGF-IR and WT NPM-ALK is associated with marked increase in NPM-ALK kinase activity compared with cotransfection of these cells with IGF-IR^{Y1131,1135,1136F} and WT NPM-ALK. The results represent one of 2 consistent experiments. (L) Coimmunoprecipitation studies in 293T cell line show that NPM-ALK^{Y338F} possesses significantly low levels of tyrosine phosphorylation. Similar to WT NPM-ALK, NPM-ALK^{Y338F} can still efficiently bind to IGF-IR. Nonetheless, in comparison to WT NPM-ALK, NPM-ALK^{Y338F} lacks the ability to induce the phosphorylation/activation of IGF-IR. (M) NPM-ALK^{Y338F} does not increase the basal level of IGF-IR kinase activity in 293T cells. The results are representative of 2 consistent experiments.

Downloaded from http://ashpublications.net/blood/article-pdf/114/2/360/1319577/zh802809000360.pdf by guest on 12 June 2024

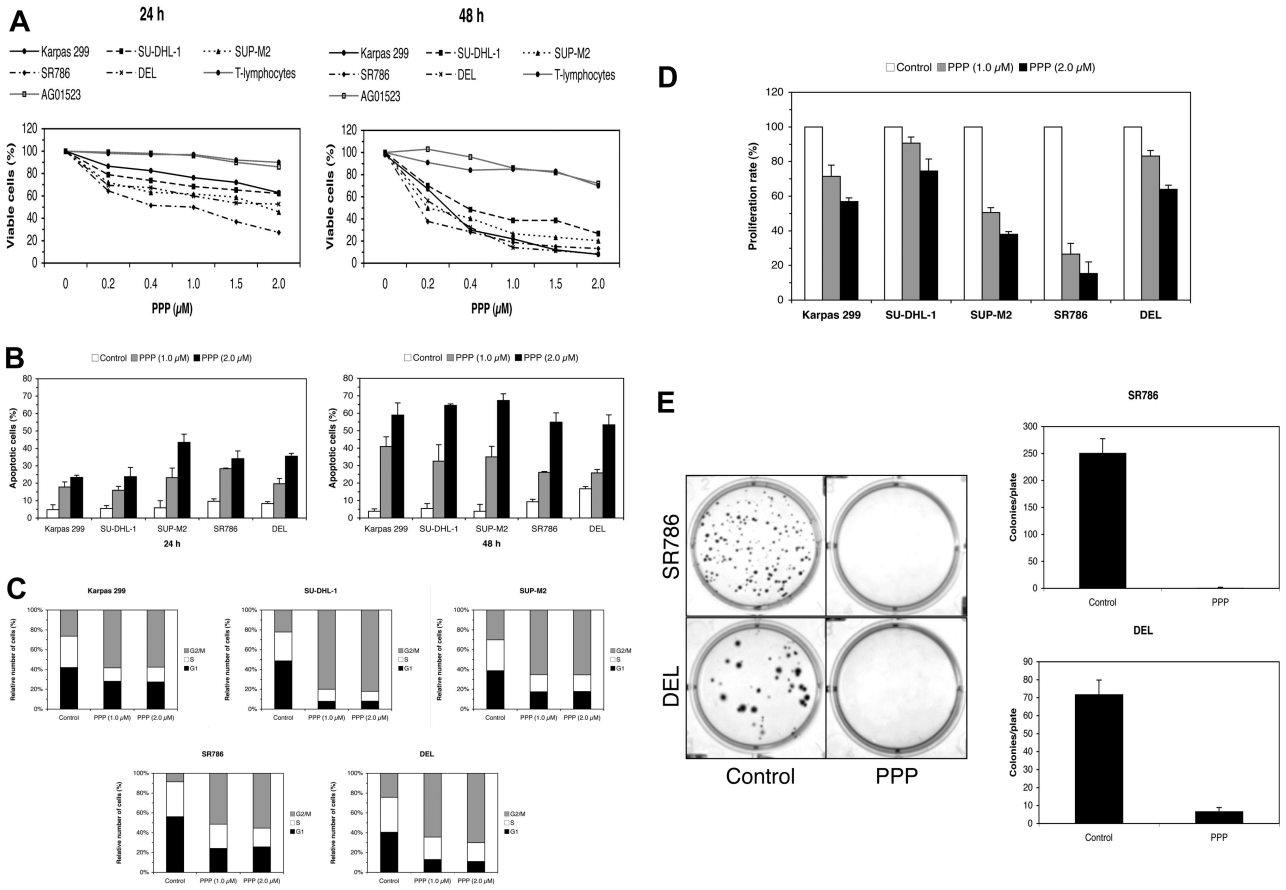

Figure 5. Selective blockade of IGF-IR signaling induces negative biologic effects in ALK$^+$ ALCL cells. (A) PPP induces a concentration- and time-dependent decrease in ALK$^+$ ALCL cell viability, as measured by exclusion of staining by trypan blue dye at 24 or 48 hours. Importantly, PPP did not induce similar effects on the cell viability of 2 human benign cell types, namely the normal T lymphocytes and the AG01523 cell line that was derived from normal skin fibroblasts. The results represent 2 consistent experiments. (B) PPP (1 μM for 24 hours) also induces a concentration- and time-dependent increase in apoptotic cell death of ALK$^+$ ALCL cells, as demonstrated by flow cytometry after staining with annexin V. The results are shown as the mean ± SD of 3 experiments. All treatment points were statistically significant compared with control untreated cells ($P < .05$). (C) Treating ALK$^+$ ALCL cells with PPP (1 μM for 24 hours) induces G_2/M-phase cell-cycle arrest. (D) PPP at 24 hours induces concentration-dependent decrease in the proliferation of ALK$^+$ ALCL cells. The decrease in cell proliferation is highly pronounced in SUP-M2 and SR786 cells, with an intermediate effect in Karpas 299 and DEL cells. The results of 3 experiments are shown as mean ± SD. Excluding SU-DHL-1 and DEL cell lines treated with PPP at 1.0 μM, all other treatments were statistically significant compared with control untreated cells ($P < .05$). (E) Treating ALK$^+$ ALCL cell lines with PPP induces a marked decrease in the potential of these cells to form colonies in soft agar. In the left panel, the effects of PPP on SR786 and DEL cell growth are shown as representative examples. Compared with the plates with control nontreated cells, the plates with treated cells show markedly decreased colony formation ($P < .001$ for SR786 and $P < .01$ for DEL). As shown in the right panel, the experiments were repeated 3 times, and the results are depicted as the mean ± SD.

cell death by 92%, 71%, and 60% above the baseline levels in the Karpas 299, SU-DHL-1, and SR786 cells, respectively. Our results also show that IGF-I stimulates the migration of serum-deprived ALK$^+$ ALCL cells (Figure 6A), as illustrated in SUP-M2, SR786, and DEL cell lines (70%, 26%, and 40.5% increase in migrating cells, respectively). Moreover, IGF-I improved the viability of serum-deprived ALK$^+$ ALCL cells (Figure 6B). The increase in the viability of serum-deprived ALK$^+$ ALCL cells could be explained by the fact that IGF-I salvaged these cells from apoptotic cell death (Figure 6C). The effects of IGF-I on cell migration, viability, and apoptosis were significantly diminished when the cells were treated with either anti-IGF-I neutralizing antibody or anti-IGF-IR blocking antibody (Figure 6A-C).

Targeting IGF-IR signaling induces significant alterations of survival proteins in ALK$^+$ ALCL cells

WB analysis confirmed that PPP induces down-regulation of pIGF-IR, with no effect on the basal level of IGF-IR protein (Figure 7A). In addition, PPP decreased IGF-IR kinase activity in a concentration-dependent manner (data not shown). These effects were associated with down-regulation of pNPM-ALK (Tyr664), pAkt (Ser473), and pSTAT3 (Tyr705; Figure 7A). PPP-induced apoptosis was also due to decreased Mcl-1 and Bcl-2 levels (Figure 7A). PPP increased cyclin B1 and decreased pCdc, with no changes in p16 levels (Figure 7A). These alterations are in agreement with the occurrence of G_2/M-phase cell-cycle arrest. The findings in downstream proteins were consistent when siRNA was used for 24 hours to specifically down-regulate IGF-IR (Figure 7B).

EMSA and ELISA studies also showed that treating the ALK$^+$ ALCL cells with PPP decreases STAT3 (Figure 7C) and increases FKHR (Figure 7D) binding to DNA. The exception was Karpas 299 cells, which showed a lower level of FKHR binding to DNA after treatment with PPP (Figure 7D). Supershift results are shown in supplemental Figure 5.

Discussion

We sought to explore a role of IGF-IR in ALK$^+$ ALCL, an aggressive type of T-cell lymphoma. One rationale for selecting this lymphoma is

Downloaded from http://ashpublications.net/blood/article-pdf/114/2/360/1319577/zh802809000360.pdf by guest on 12 June 2024

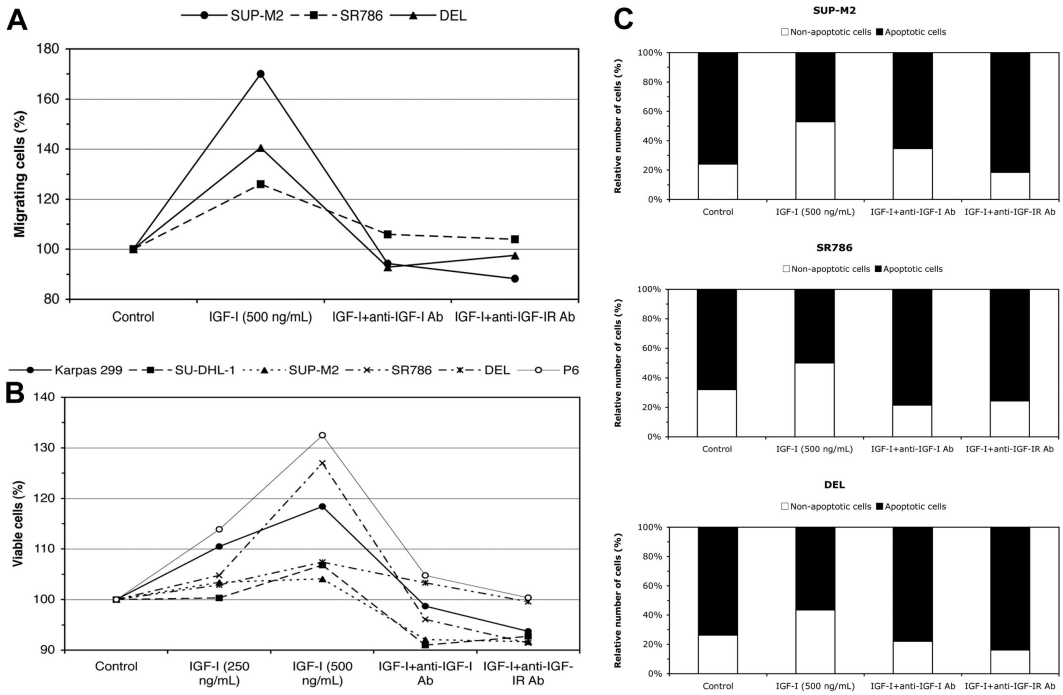

Figure 6. Effects of stimulation by IGF-I and specific blockade of IGF-IR on ALK+ ALCL cells. To confirm the findings of inhibition of IGF-IR signaling by PPP in ALK+ ALCL cells and to rule out that these findings were due to nonspecific effects, 3 specific approaches were used that involved stimulating the cells with IGF-I for 24 hours after growing the cells in serum-free RPMI medium for 3 hours. (A) Stimulation of IGF-IR signaling by IGF-I promotes serum-deprived ALK+ ALCL cell migration, which is abrogated by treating the cells with anti–IGF-I neutralizing antibody or anti–IGF-IR blocking antibody. The results are representative of 2 consistent experiments. (B) Stimulation of IGF-IR signaling by IGF-I induces a concentration-dependent increase in the viability of serum-deprived ALK+ ALCL and P6 (positive control) cells. This effect was also reversed when specific antibodies were used to neutralize IGF-I or to block IGF-IR. The results are representative of 2 consistent experiments. (C) The increase in cell viability could be due to a decrease in the apoptosis of serum-deprived ALK+ ALCL cells. Treating the cells with either anti–IGF-I neutralizing antibody or anti–IGF-IR blocking antibody similarly reversed this effect of IGF-I. The results are representative of 2 consistent experiments.

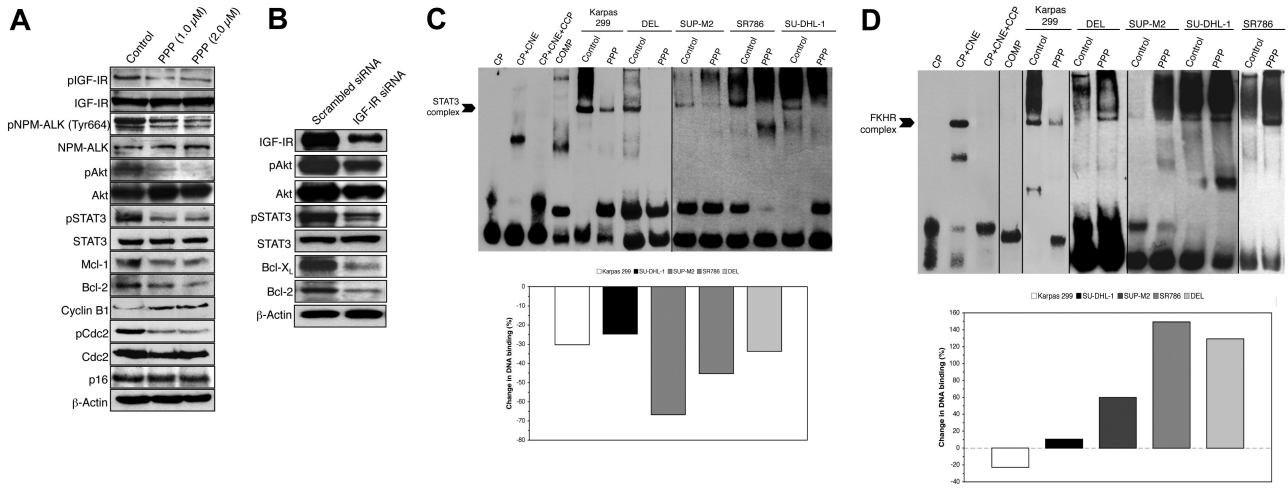

Figure 7. Targeting of IGF-IR induces significant effects on downstream survival proteins in ALK+ ALCL cells. To explore possible explanations for the negative effects of down-regulation of IGF-IR signaling on ALK+ ALCL, the effect of selective blockade of IGF-IR by PPP on proteins downstream of IGF-IR was studied. These proteins are also known to significantly contribute to the pathogenesis of ALK+ ALCL. (A) WB (Karpas 299 cell line is shown as a representative example) confirmed that at 24 hours, PPP induces marked down-regulation of pIGF-IR, without a noticeable change in IGF-IR levels. The decrease in pIGF-IR is associated with decreases in pNPM-ALK (Tyr664), pAkt (Ser473), and pSTAT3 (Tyr705). In addition, PPP induces significant decreases in the antiapoptotic proteins Mcl-1 and Bcl-2. Furthermore, PPP induces a notable increase and decrease in the cell-cycle regulatory proteins cyclin B1 and pCdc, respectively. Changes are not seen in p16 and Cdc. The effects of PPP on the cell cycle regulatory proteins are consistent with the occurrence of G_2/M-phase cell-cycle arrest. (B) We also used specific targeting of IGF-IR by siRNA to confirm some of the results and to rule out the possibility of nonspecific effects of the pharmacologic agent PPP. IGF-IR siRNA decreased pAkt, pSTAT3, Bcl-X_L, and Bcl-2 levels. To further explore the mechanisms by which IGF-IR induces its oncogenic effects in ALK+ ALCL, the binding of STAT3 (C) and FKHR (D) to DNA was studied by using 2 different techniques, namely EMSA (top panels) and ELISA (bottom panels), after treatment with PPP (2 μM for 24 hours). (C) PPP significantly decreases STAT3 binding to DNA in the 5 ALK+ ALCL cell lines. The difference in the migration of the STAT3-DNA binding band between the control and the ALK+ ALCL cells could be explained by the difference in the target sequence. A vertical line has been inserted to indicate prepositioned gel lanes. (D) In contrast to its effect on STAT3, PPP enhances FKHR binding to DNA in SU-DHL-1, SUP-M2, SR786, and DEL cells. These results are in agreement with PPP-induced cell death of these cells. Vertical lines have been inserted to indicate repositioned gel lanes. The controls (CP, control probe; CNE, control nuclear extract; CCP, cold control probe; COMP, competition) confirm that the reagents performed properly.

Downloaded from http://ashpublications.net/blood/article-pdf/114/2/360/1319577/zh802809000360.pdf by guest on 12 June 2024

that full-length ALK is a member of the insulin receptor superfamily of tyrosine kinases. Members of this family demonstrate structural homology because they contain the Y*XXX*YY motif within the activation loop of their kinase domains. For instance, the activation loop of IGF-IR contains Tyr1131, Tyr1135, and Tyr1136, and that of ALK contains Tyr1278, Tyr1282, and Tyr1283 (Tyr338, Tyr342, and Tyr343 in NPM-ALK). Our results show that IGF-IR is universally expressed in ALK$^+$ ALCL cell lines and in the majority of human tumor samples. Importantly, IGF-IR expression is significantly more pronounced in ALK$^+$ ALCL cell lines compared with benign human T lymphocytes. IGF-I, the primary ligand of IGF-IR, is also widely expressed in these cell lines and primary tumors.

NPM-ALK is a constitutively active protein tyrosine kinase with significant oncogenic potential.[46] To induce its oncogenic effects, NPM-ALK interacts with several proteins that regulate cell survival and growth.[47] Our results illustrate novel reciprocal functional interactions between NPM-ALK and IGF-IR. These interactions were essentially based on the physical association between the 2 kinases. Deletion of the NPM portion of NPM-ALK did not affect its binding to IGF-IR. It is likely that the C terminus portion of NPM-ALK plays a crucial role in its association with IGF-IR, because deletion of this segment totally abrogated the binding between the 2 kinases. We further characterized the binding between IGF-IR and NPM-ALK by focusing on the 4 tyrosine residues present within the C terminus of NPM-ALK. One rationale for this approach was that previous studies have demonstrated that some of these residues bind and interact with crucial downstream targets of NPM-ALK.[53,54] In addition, when we down-regulated IGF-IR, there was significant decrease in the phosphorylation levels of 2 tyrosine residues, Tyr646 and Tyr664, located within the C terminus of NPM-ALK. Substitution of Tyr644 or Tyr664 with phenylalanine significantly decreased, but not completely abolished, the binding of NPM-ALK to IGF-IR. In contrast, we could not detect similar effects when Tyr567 or Tyr646 of NPM-ALK was mutated. These findings indicate that IGF-IR simultaneously binds to Tyr644 and Tyr664 of NPM-ALK. However, the possibility that IGF-IR might also bind to NPM-ALK through other amino acid residues cannot be completely excluded.

IGF-IR appears to function as a substrate to NPM-ALK. In agreement with this notion, specific targeting of ALK by siRNA decreased phosphorylated IGF-IR in ALK$^+$ ALCL cell lines. Furthermore, NPM-ALK induced up-regulation of phosphorylated IGF-IR, and it is important to emphasize that the kinase-defective NPM-ALK failed to induce a similar effect. These findings were consistent in 3 different cell types as was shown when P6, Jurkat, and the ALK$^+$ ALCL cell line DEL were transfected with WT NPM-ALK or its kinase-defective mutant. Further analysis identified the Tyr338 residue of NPM-ALK to play a significant role in the phosphorylation of IGF-IR. NPM-ALK^{Y338F} possessed significantly less tyrosine phosphorylation levels and kinase activity compared with WT NPM-ALK. Although it retained significant ability to bind to IGF-IR, NPM-ALK^{Y338F} could not maintain the phosphorylation status or increase the kinase activity of IGF-IR. Tyr338 is the first tyrosine in the Y*XXX*YY motif of the activation loop of NPM-ALK. Recently, Tartari et al proposed that this residue is necessary for the NPM-ALK kinase domain to adopt a fully active conformation.[55] In addition, similar to our findings in IGF-IR, they showed that NPM-ALK^{Y338F} demonstrated much less ability to phosphorylate important oncogenic proteins, including STAT3, Akt, and MAPK.[55] We have noticed that, compared with the present study where the kinase activity of NPM-ALK^{Y338F} decreased to approximately 60% of the basal level observed in WT NPM-ALK, Tartari et al demonstrated an NPM-ALK^{Y338F} kinase activity of only 25% of its level in WT NPM-ALK.[55] This discrepancy could be explained by the differences in some of the experimental conditions including the transfection protocols, cell lines, and kinase activity detection methods.

Targeting of IGF-IR by PPP reciprocally decreased the phosphorylation levels of NPM-ALK, providing evidence to further support a positive feedback mechanism between IGF-IR and NPM-ALK. PPP is a cyclolignan that induces activation loop-specific inhibition of the tyrosine phosphorylation of IGF-IR.[7,52] Although we cannot completely exclude that the effect of PPP was at least partially due to a direct interaction with NPM-ALK, specific inhibition of IGF-IR by siRNA also induced a marked decrease in phosphorylated NPM-ALK at Tyr646 and Tyr664, which provides strong evidence to support a direct role of IGF-IR in maintaining the phosphorylation status of NPM-ALK. Furthermore, when the ALK$^+$ ALCL cell line DEL was transfected with WT IGF-IR, the basal level of phosphorylated NPM-ALK was markedly increased. In addition, cotransfection of R$^-$ cells with WT NPM-ALK and WT IGF-IR was associated with marked increase in NPM-ALK kinase activity. These effects were not seen when the same cells were transfected with IGF-IR^{Y1131,1135,1136F} mutant that demonstrated markedly reduced kinase activity. In line with these findings, when ALK siRNA decreased pAkt and pSTAT3 levels, treating the ALK$^+$ ALCL with IGF-I reversed this decrease. Notably, treating the ALK$^+$ ALCL cells with IGF-I induced significant increase in NPM-ALK kinase activity. Of functional interest is that Tyr646 and Tyr664 residues that appear to interact with IGF-IR are located within the C terminus portion of NPM-ALK. Because we have also found that IGF-IR binds to Tyr664 of NPM-ALK, most likely this amino acid residue contributes significantly to the functional interactions between the 2 kinases and to subsequent downstream signaling. In support of the mechanistic relevance of Tyr664 to the oncogenic effects of NPM-ALK, Bai et al have previously demonstrated that NPM-ALK binds to the downstream modulator phospholipase C-γ through Tyr664, which allows NPM-ALK to induce transformation effects.[53]

Unlike full-length ALK, NPM-ALK is entirely intracellular and lacks an extracellular domain. Collectively, our findings suggest a novel model in which IGF-IR would function as an extracellular domain to maintain the phosphorylation status of NPM-ALK in order for it to subsequently activate/phosphorylate downstream proteins. Similar to our findings in IGF-IR, previous studies have suggested that some cytoplasmic and membrane-associated tyrosine kinases are able to maintain the phosphorylation/activation status of chimeric proteins with tyrosine kinase activity such as BCR-ABL and NPM-ALK.[56-58]

Next, we found that selective or specific antagonism of IGF-IR signaling leads to negative biologic affects in ALK$^+$ ALCL cells. These negative effects included G_2/M-phase cell cycle arrest, a previously reported effect of PPP.[34] It is important to emphasize that the blockade of IGF-IR by PPP failed to induce negative biologic effects in 2 benign human cell types including skin fibroblasts and T lymphocytes. These findings are in agreement with the recently reported lack of significant untoward effects of some of the IGF-IR inhibitors that are currently used in clinical trials of patients with solid tumors.[28] The significant biologic role of IGF-IR in this lymphoma also was highlighted when serum-deprived ALK$^+$ ALCL cells were stimulated with IGF-I, which promoted the migration of these cells. The stimulatory effect of IGF-I on the migration of ALK$^+$ ALCL cells could represent one factor contributing to the known tendency of these cells to migrate and localize in the lymph node sinuses. Furthermore, treating serum-deprived ALK$^+$ ALCL cells with IGF-I increased their viability and salvaged a proportion of these cells from apoptotic cell death. Of particular importance is that the anti-IGF-IR blocking antibody reversed the effects of

Downloaded from http://ashpublications.net/blood/article-pdf/114/2/360/1319577/zh802809000360.pdf by guest on 12 June 2024

IGF-I, which should exclude the possibility of stimulation of the insulin receptor by IGF-I.

IGF-IR induces its effects via phosphorylation of downstream proteins that regulate cell survival, such as Akt, STAT3, and FKHR.[3,5,7] Aberrancies in these proteins have been shown to occur and to contribute to the pathogenesis of ALK+ ALCL.[59-61] Selective and specific blockade of IGF-IR significantly decreased the levels of phosphorylated/activated Akt and STAT3. This blockade also decreased STAT3 and increased FKHR binding to DNA in ALK+ ALCL cell lines. Moreover, targeting IGF-IR induced pronounced alterations in apoptosis and cell-cycle regulatory proteins, including Bcl-2, Bcl-X_L, Mcl-1, cyclin B1, and pCdc. These findings add to confirm the important role of IGF-IR in ALK+ ALCL and identify some of the possible mechanisms by which inhibition of IGF-IR induces negative biologic effects in these cells.

We detected the expression of IGF-IR in 60% of a limited number of ALK-negative ALCL primary tumors. In addition to the ALK-negative T-cell lymphoid cell line Jurkat, we also found the expression of IGF-IR in the ALK-negative ALCL cell line Mac-2A (data not shown). When we tested the effect of PPP, we detected a notable decrease in the viability of the Mac-2A cell line (data not shown). These observations suggest that IGF-IR may also play a role in other types of T-cell lymphoma that lack the expression of NPM-ALK. Nonetheless, similar to several solid tumors that have frequent expression and established oncogenic role of IGF-IR, a potential role of IGF-IR in these lymphomas must be independent of NPM-ALK. An interesting observation is that none of the ALK-negative tumors expressed IGF-I. Although the number of the ALK-negative tumors included in this study is relatively small, the lack of expression of IGF-I by these tumors and its frequent expression by the ALK+ ALCL cell lines and primary tumors could argue that NPM-ALK might play a role in regulating the expression of IGF-I in a fashion similar to what has been recently described for BCR-ABL by Lakshmikuttyamma et al, who reported the regulation of IGF-I system by BCR-ABL in the chronic myeloid leukemia (CML) cell line K562.[62] However, the expression and secretion of IGF-I by BCR-ABL-positive cells is not universal, as we have failed to detect the expression and/or release of IGF-I by 3 other established BCR-ABL-positive cell lines. These results in CML cell lines are somehow similar to our findings in some of the ALK+ ALCL cell lines, such as Karpas 299 cells that lacked the expression of IGF-I in spite of harboring the NPM-ALK chimeric protein, and suggest that in addition to NPM-ALK or BCR-ABL oncogenic proteins, other factors could still play important roles in the regulation of IGF-I expression by these cells.

The results presented in this paper were obtained from experiments performed in 5 previously established ALK+ ALCL cell lines. Only the Karpas 299 cell line lacked the expression of IGF-I protein and demonstrated a decrease in FKHR binding to DNA after inhibition of IGF-IR. It is possible that these effects stem from the role that IGF-IR plays in maintaining the normal homeostasis of living cells, and they could represent a counterbalance by which neoplastic cells attempt to antagonize survival signaling.[64] Regardless, the net effect of targeting IGF-IR in Karpas 299 cells was similar to the other cell lines, ie, cell death.

In conclusion, herein we identify a new role for IGF-IR in cancer, namely that in the pathogenesis of T-cell ALK+ ALCL. We also reveal novel association and reciprocal functional collaboration between IGF-IR and NPM-ALK. These findings are expected to expand the current understanding of the biology of IGF-IR, NPM-ALK, and ALK+ ALCL. The possibility of a significant role of IGF-IR in other types of malignant lymphoma also needs to be extensively investigated. As targeting of IGF-IR signaling is currently being examined in clinical trials, the identified role of IGF-IR in ALK+ ALCL may have a significant therapeutic impact on the treatment of this aggressive lymphoma in the near future.

Acknowledgments

The authors are grateful to Kim-Anh Vu and Dawn Chalaire for their valuable help with the preparation of this manuscript. This work is supported by CA114395 grant from the National Institutes of Health and by the Physician Scientist Program Award from M. D. Anderson Cancer Center to H.M.A.

Authorship

Contribution: P.S. and H.M.A. designed research; P.S., Q.L., A.S.I., L.C.Y., and H.M.A. performed research and collected data; P.S. and H.M.A. interpreted and analyzed data; R.L., L.W.K., R.J.F., and H.M.A. provided important experimental and analytical tools; and P.S. and H.M.A. wrote the paper.

Conflict-of-interest disclosure: The authors declare no competing financial interests.

Correspondence: Hesham M. Amin, Department of Hematopathology, Unit 72, The University of Texas M. D. Anderson Cancer Center, 1515 Holcombe Blvd, Houston, TX 77030; e-mail: hamin@mdanderson.org.

References

1. Ullrich A, Gray A, Tam AW, et al. Insulin-like growth factor I receptor primary structure: comparison with insulin receptor suggests structural determinants that define functional specificity. *EMBO J.* 1986;5:2503-2512.
2. De Meyts P, Whittaker J. Structural biology of insulin and IGF1 receptors: implications for drug design. *Nat Rev Drug Discov.* 2002;1:769-783.
3. Zong CS, Chan J, Levy DE, Horvath C, Sadowski HB, Wang LH. Mechanism of STAT3 activation by insulin-like growth factor I receptor. *J Biol Chem.* 2000;275:15099-15105.
4. Gual P, Baron V, Lequoy V, Van Obberghen E. Interaction of Janus kinases JAK-1 and JAK-2 with the insulin receptor and the insulin-like growth factor-1 receptor. *Endocrinology.* 1998; 139:884-893.
5. Nakae J, Barr V, Accili D. Differential regulation of gene expression by insulin and IGF-1 receptors correlates with phosphorylation of a single amino acid residue in the forkhead transcription factor FKHR. *EMBO J.* 2000;19:989-996.
6. Galetic I, Andjelkovic M, Meier R, Brodbeck D, Park J, Hemmings BA. Mechanism of protein kinase B activation by insulin/insulin-like growth factor-1 revealed by specific inhibitors of phosphoinositide 3-kinase—significance for diabetes and cancer. *Pharmacol Ther.* 1999;82:409-425.
7. Vasilcanu D, Girnita A, Girnita L, Vasilcanu R, Axelson M, Larsson O. The cyclolignan PPP induces activation loop-specific inhibition of tyrosine phosphorylation of the insulin-like growth factor-1 receptor. Link to phosphatidyl inositol-3 kinase/Akt apoptotic pathway. *Oncogene.* 2004; 23:7854-7862.
8. Criswell T, Beman M, Araki S, et al. Delayed activation of insulin-like growth factor-1 receptor/Src/MAPK/Erg-1 signaling regulates clusterin expression, a pro-survival factor. *J Biol Chem.* 2005; 280:14212-14221.
9. Baserga R, Sell C, Porcu P, Rubini M. The role of the IGF-I receptor in the growth and transformation of mammalian cells. *Cell Prolif.* 1994;27:63-71.
10. Sell C, Rubini M, Rubin R, Liu JP, Efstratiadis A, Baserga R. Simian virus 40 large tumor antigen is unable to transform mouse embryonic fibroblasts lacking type 1 insulin-like growth factor receptor. *Proc Natl Acad Sci U S A.* 1993;90:11217-11221.
11. Samani AA, Yakar S, LeRoith D, Brodt P. The role of the IGF system in cancer growth and metastasis: overview and recent insights. *Endocr Rev.* 2007;28:20-47.
12. van Golen CM, Schwab TS, Kim B, et al. Insulin-like growth factor-I receptor expression regulates neuroblastoma metastasis to bone. *Cancer Res.* 2006;66:6570-6578.
13. Tang Y, Zhang D, Fallavollita L, Brodt P. Vascular

Downloaded from http://ashpublications.net/blood/article-pdf/114/2/360/1319577/zh802809000360.pdf by guest on 12 June 2024

endothelial growth factor C expression and lymph node metastasis are regulated by the type I insulin-like growth factor receptor. *Cancer Res.* 2003;63:1166-1171.

14. Guvakova MA, Adams JC, Boettiger D. Functional role of α-actinin, PI 3-kinase and MEK1/2 in insulin-like growth factor I receptor kinase regulated motility of human breast carcinoma cells. *J Cell Sci.* 2002;115:4149-4165.
15. Mauro L, Bartucci M, Morelli C, Ando S, Surmacz E. IGF-I receptor-induced cell-cell adhesion of MCF-7 breast cancer cells requires the expression of junction protein ZO-1. *J Biol Chem.* 2001; 276:39892-39897.
16. Chernicky CL, Yi L, Tan H, Gan SU, Ilan J. Treatment of human breast cancer cells with antisense RNA to the type I insulin-like growth factor receptor inhibits cell growth, suppresses tumorigenesis, alters the metastatic potential, and prolongs survival in vivo. *Cancer Gene Ther.* 2000;7:384-395.
17. Lopez T, Hanahan D. Elevated levels of the IGF-I receptor convey invasion and metastatic capability in a mouse model of pancreatic islet tumorigenesis. *Cancer Cell.* 2002;1:339-353.
18. Adachi Y, Lee CT, Coffee K, et al. Effects of genetic blockade of the insulin-like growth factor receptor in human colon cancer cell lines. *Gastroenterology.* 2002;123:1191-1204.
19. Dunn SE, Ehrlich M, Sharp NJ, et al. A dominant negative mutant of the insulin-like growth factor-I receptor inhibits the adhesion, invasion, and metastasis of breast cancer. *Cancer Res.* 1998;58: 3353-3361.
20. Hellawell GO, Turner GD, Davies DR, Poulsom R, Brewster SF, Macaulay VM. Expression of the type 1 insulin-like growth factor receptor is upregulated in primary prostate cancer and commonly persists in metastatic disease. *Cancer Res.* 2002;62:2942-2950.
21. Maloney EK, McLaughlin JL, Dagdigian NE, et al. An anti-insulin-like growth factor I receptor antibody that is a potent inhibitor of cancer cell proliferation. *Cancer Res.* 2003;63:5073-5083.
22. Lee CT, Park KH, Adachi Y, et al. Recombinant adenoviruses expressing dominant negative insulin-like growth factor-I receptor demonstrate antitumor effects on lung cancer. *Cancer Gene Ther.* 2003;10:57-63.
23. Burfeind P, Chernicky CL, Rininsland F, Ilan J, Ilan J. Antisense RNA to the type I insulin-like growth factor receptor suppresses tumor growth and prevents invasion by rat prostate cancer cells in vivo. *Proc Natl Acad Sci U S A.* 1996;93:7263-7268.
24. Singleton JR, Randolph AE, Feldman EL. Insulin-like growth factor I receptor prevents apoptosis and enhances neuroblastoma tumorigenesis. *Cancer Res.* 1996;56:4522-4529.
25. Hofmann F, Garcia-Echeverria C. Blocking the insulin-like growth factor-I receptor as a strategy for targeting cancer. *Drug Discov Today.* 2005;10: 1041-1047.
26. Surmacz E. Growth factor receptors as therapeutic targets: strategies to inhibit the insulin-like growth factor I receptor. *Oncogene.* 2003;22:6589-6597.
27. Baserga R. Controlling IGF-receptor function: a possible strategy for tumor therapy. *Trends Biotechnol.* 1996;14:150-152.
28. Haluska P, Shaw HM, Batzel GN, et al. Phase I dose escalation study of the anti insulin-like growth factor-I receptor monoclonal antibody CP-751,871 in patients with refractory solid tumors. *Clin Cancer Res.* 2007;13:5834-5840.
29. McCubrey JA, Steelman LS, Mayo MW, Algate PA, Dellow RA, Kaleko M. Growth-promoting effects of insulin-like growth factor-1 (IGF-1) on hematopoietic cells: overexpression of introduced IGF-1 receptor abrogates interleukin-3 dependency of murine factor-dependent cells by a ligand-dependent mechanism. *Blood.* 1991;78:921-929.
30. Reiss K, Porcu P, Sell C, Pietrzkowski Z, Baserga R. The insulin-like growth factor 1 receptor is required for the proliferation of hemopoietic cells. *Oncogene.* 1992;7:2243-2248.
31. Bertrand FE, Steelman LS, Chappell WH, et al. Synergy between an IGF-1R antibody and Raf/MEK/ERK and PI3K/Akt/mTOR pathway inhibitors in suppressing IGF-1R-mediated growth in hematopoietic cells. *Leukemia.* 2006;20:1254-1260.
32. Walsh PT, Smith LM, O'Connor R. Insulin-like growth factor-1 activates Akt and Jun N-terminal kinases (JNKs) in promoting the survival of T lymphocytes. *Immunology.* 2002;107:461-471.
33. Menu E, Jernberg-Wiklund H, Stromberg T, et al. Inhibiting the IGF-1 receptor tyrosine kinase with the cyclolignan PPP: an in vitro and in vivo study in the 5T33MM mouse model. *Blood.* 2006;107:655-660.
34. Stromberg T, Ekman S, Girnita L, et al. IGF-1 receptor tyrosine kinase inhibition by the cyclolignan PPP induces G2/M-phase accumulation and apoptosis in multiple myeloma cells. *Blood.* 2006;107:669-678.
35. Mitsiades CS, Mitsiades NS, McMullan CJ, et al. Inhibition of insulin-like growth factor receptor-1 tyrosine kinase activity as a therapeutic strategy for multiple myeloma, other hematologic malignancies, and solid tumors. *Cancer Cell.* 2004;5:221-230.
36. Iwahara T, Fujimoto J, Wen D, et al. Molecular characterization of ALK, a receptor tyrosine kinase expressed specifically in the nervous system. *Oncogene.* 1997;14:439-449.
37. Morris SW, Naeve C, Mathew P, et al. ALK, the chromosome 2 gene locus altered by the t(2;5) in non-Hodgkin's lymphoma, encodes a novel neural receptor tyrosine kinase that is highly related to leukocyte tyrosine kinase (LTK). *Oncogene.* 1997;14:2175-2188.
38. Delsol G, Falini B, Muller-Hermelink HK, et al. Anaplastic large cell lymphoma (ALCL), ALK-positive. In: Swerdlow SH, Campo E, Harris NL, et al, eds. *WHO Classification of Tumours of Haematopoietic and Lymphoid Tissues.* 4th ed. Lyon, France: International Agency for Research on Cancer (IARC); 2008:312-316.
39. Morris SW, Kirstein MN, Valentine MB, et al. Fusion of a kinase gene, ALK, to a nucleolar protein gene, NPM, in non-Hodgkin's lymphoma. *Science.* 1994;263:1281-1284.
40. Shiota M, Fujimoto J, Semba T, Satoh H, Yamamoto T, Mori S. Hyperphosphorylation of a novel 80 kDa protein-tyrosine kinase similar to Ltk in a human Ki-1 lymphoma cell line, AMS3. *Oncogene.* 1994;9:1567-1574.
41. Shiota M, Nakamura S, Ichinohasama R, et al. Anaplastic large cell lymphomas expressing the novel chimeric protein p80NPM/ALK: a distinct clinicopathologic entity. *Blood.* 1995;86:1954-1960.
42. Falini B, Pileri S, Zinzani PL, et al. ALK$^+$ lymphoma: clinico-pathological findings and outcome. *Blood.* 1999;93:2697-2706.
43. Brugieres L, Le Deley MC, Pacquement H, et al. CD30$^+$ anaplastic large-cell lymphoma in children: analysis of 82 patients enrolled in two consecutive studies of the French Society of Pediatric Oncology. *Blood.* 1998;92:3591-3598.
44. Brugieres L, Quartier P, Le Deley MC, et al. Relapses of childhood anaplastic large-cell lymphoma: treatment results in a series of 41 children—a report from the French Society of Pediatric Oncology. *Ann Oncol.* 2000;11:53-58.
45. Laver JH, Kraveka JM, Hutchinson RE, et al. Advanced-stage large-cell lymphoma in children and adolescents: results of a randomized trial incorporating intermediate-dose methotrexate and high-dose cytarabine in the maintenance phase of the APO regimen: a Pediatric Oncology Group phase III trial. *J Clin Oncol.* 2005;23:541-547.
46. Fujimoto J, Shiota M, Iwahara T, et al. Characterization of the transforming activity of p80, a hyperphosphorylated protein in a Ki-1 lymphoma cell line with chromosomal translocation t(2;5). *Proc Natl Acad Sci U S A.* 1996;93:4181-4186.
47. Amin HM, Lai R. Pathobiology of ALK$^+$ anaplastic large-cell lymphoma. *Blood.* 2007;110:2259-2267.
48. Liu J-P, Baker J, Perkins AS, Robertson EJ, Efstratiadis A. Mice carrying null mutations of the genes encoding insulinlike growth factor (Igf-1) and type 1 IGF receptor (Igf1r). *Cell.* 1993;75:59-72.
49. Pietrzkowski Z, Lammers R, Carpenter G, et al. Constitutive expression of insulin-like growth factor 1 and insulin-like growth factor 1 receptor abrogates all requirements for exogenous growth factors. *Cell Growth Differ.* 1992;3:199-205.
50. Rosengren L, Vasilcanu D, Vasilcanu R, et al. IGF-1R tyrosine kinase expression and dependence in clones of IGF-1R knockout cells (R-). *Biochem Biophys Res Commun.* 2006;347:1059-1066.
51. Qiu L, Lai R, Lin Q, et al. Autocrine release of interleukin-9 promotes Jak3-dependent survival of ALK$^+$ anaplastic large-cell lymphoma cells. *Blood.* 2006;108:2407-2415.
52. Girnita A, Girnita L, del Prete F, Bartolazzi A, Larsson O, Axelson M. Cyclolignans as inhibitors of the insulin-like growth factor-1 receptor and malignant cell growth. *Cancer Res.* 2004;64:236-242.
53. Bai R-Y, Dieter P, Peschel C, Morris SW, Duyster J. Nucelophosmin-anaplastic lymphoma kinase of large-cell anaplastic lymphoma is a constitutively active tyrosine kinase that utilizes phospholipase C-γ to mediate its mitogenicity. *Mol Cell Biol.* 1998;12:6951-6961.
54. Chikamori M, Fujimoto J, Tokai-Nishizumi N, Yamamoto T. Identification of multiple SNT-binding sites on NPM-ALK oncoprotein and their involvement in cell transformation. *Oncogene.* 2007;26:2950-2954.
55. Tartari CJ, Gunby RH, Coluccia AML, et al. Characterization of some molecular mechanisms governing autoactivation of the catalytic domain of the anaplastic lymphoma kinase. *J Biol Chem.* 2008;283:3743-3750.
56. Amin HM, Medeiros LJ, Ma Y, et al. Inhibition of JAK3 induces apoptosis and decreases anaplastic lymphoma kinase activity in anaplastic large cell lymphoma. *Oncogene.* 2003;22:5399-5407.
57. Cussac D, Greenland C, Roche S, et al. Nucleophosmin-anaplastic lymphoma kinase of anaplastic large-cell lymphoma recruits, activates, and uses pp60$^{c\text{-}src}$ to mediate its mitogenicity. *Blood.* 2004;103:1464-1471.
58. Meyn MA, Wilson MB, Abdi FA, et al. Src family kinases phosphorylate the Bcr-Abl SH3-SH2 region and modulate Bcr-Abl transforming activity. *J Biol Chem.* 2006;281:30907-30916.
59. Amin HM, McDonnell TJ, Ma Y, et al. Selective inhibition of STAT3 induces apoptosis and G_1 cell cycle arrest in ALK-positive anaplastic large cell lymphoma. *Oncogene.* 2004;23:5426-5434.
60. Rassidakis GZ, Feretzaki M, Atwell C, et al. Inhibition of Akt increases p27^{Kip1} levels and induces cell cycle arrest in anaplastic large cell lymphoma. *Blood.* 2005;105:827-829.
61. Gu T-L, Tothova Z, Scheijen B, Griffin JD, Gilliland DG, Sternberg DW. NPM-ALK fusion kinase of anaplastic large-cell lymphoma regulates survival and proliferative signaling through modulation of FOXO3a. *Blood.* 2004;103:4622-4629.
62. Lakshmikuttyamma A, Pastural E, Takahashi N, et al. Bcr-Abl induces autocrine IGF-1 signaling. *Oncogene.* 2008;27:3831-3844.
63. Shi P, Chandra J, Sun X, et al. Inhibition of IGF-IR tyrosine kinase induces apoptosis and cell cycle arrest in imatinib-resistant chronic myeloid leukemia cells *J Cell Mol Med.* Prepublished online June 5, 2009, as DOI 10.1111/j.1582-4934.2009.00795.X.
64. Baserga R. The contradictions of the insulin-like growth factor 1 receptor. *Oncogene.* 2000;19: 5574-5581.

Downloaded from http://ashpublications.net/blood/article-pdf/114/2/360/1319577/zh802809000360.pdf by guest on 12 June 2024